IOP Conference Series: Earth and Environmental Science

PAPER • **OPEN ACCESS**

Study on Thermal Stability of Hypereutectic Surfacing Alloy Fe2B Hard Phase

To cite this article: Zhen Ma *et al* 2018 *IOP Conf. Ser.: Earth Environ. Sci.* **199** 052051

Study on Thermal Stability of Hypereutectic Surfacing Alloy Fe_2B Hard Phase

Zhen Ma[1], Liting Mu[1], Jun Wang[2], Minghui Zhuang[1] and Muqin Li[1*]

[1] School of Materials Science and Engineering, Jiamusi University, Jiamusi, Heilongjiang, 154007, PR China

[2] School of Aeronautics and Astronautics, Tianjin Sino-Germen University of Applied Sciences, Tianjin, 300350, PR China

[*]Corresponding author's e-mail: jmsdxmz@163.com

Abstract. The microstructure properties of high-boron surfacing and the thermal stability of Fe_2B was investigated. Each of the specimens was characterized by metallographic techniques. Phase analysis of alloy was performed by X-ray diffraction. The results show that when the carbon content was 0.13 wt%, the weld surfacing structure was blocky and rod-shaped Fe_2B+Fe. When the carbon content was 0.57 wt%, the weld structure was a bulk Fe_2B and eutectic fishbone Fe_2B, and a chrysanthemum-like $Fe_3(B,C)$. When the carbon content increased to 1.0 wt%, the fishbone tissue disappeared, and the eutectic structure consisted of chrysanthemum-like tissue. The structure was blocky Fe_2B and eutectic structure chrysanthemum $Fe_3(B,C)$. After heat treatment, the microstructure of Fe_2B hard phase in the weld microstructure did not change, and kept block and a strip shape. Due to the high temperature effect, the eutectic fish bone Fe_2B+γ-Fe and the eutectic chrysanthemum $Fe_3(B,C)$+γ-Fe between the Fe_2B were converted into Fe_2B. Fe_2B hard phase has good thermal stability.

1. Introduction

High temperature wear and tear leads to unacceptably high industrial production costs every year. It is imperative to research and promote high-temperature wear-resistant materials to reduce high costs. At present, high chromium cast iron is used as the main iron-based high-temperature wear-resistant material for metallurgy and cement industry[1-3]. The main reason is that the cost of high chromium cast iron is relatively low, and the weldability and formability are good. The various types of alloy steel parts was repaired by high-chromium and high-carbon wear-resistant materials and extend the service life of parts to varying degrees. Due to the limitation of the properties of the high-chromium and high-carbon wear-resistant materials, the stability of strengthened phase under high temperature conditions is easy to decompose and the wear resistance of the material is reduced. With the increase of the cost of wear-resistant materials and the shortage of precious alloy resources, people are forcing people to seek wear-resistant materials with higher cost performance. People have developed high-boron high-temperature wear-resistant alloy materials, and boride as a wear-resistant phase of new iron-based wear-resistant materials. The mechanical properties and wear properties of high boron iron based wear resistant materials depend on their microstructure and chemical composition[1-12]. To achieve impact resistance, a good ductility and good interfacial carbide-matrix bonding is necessary[13]. Hard phase and high hardness are important for wear resistance. It is especially important to ensure that the hardness of the hard phase and the hardness of the matrix is higher than

the hardness of the abrasive[14-18]. For temperature resistance and oxidation resistance, boride strengthening is most suitable in iron-based alloy materials.[19-20]. In view of the above situation, in order to apply high-boron iron-based surfacing wear-resistant alloy materials to industrial and mining enterprises, it is necessary to verify the thermal stability of boride.

2. Experimental materials and methods

With the arcing-wire GTAW surfacing method, the surfacing layer was prepared on steel plate of Q235 of 150 mm × 75 mm × 10 mm. The welding wire is three sets of high-boron metal powder cored wire with different carbon content. The wire diameter is 1.6 mm and the filling rate is 25 %. Optimized welding process parameters are: main arc voltage 22 V, main arc current 120 A, auxiliary arc current 160 A, wire feeding speed 40 mm/s, welding speed 5.5 mm/s, thickness of surfacing layer 5 mm, the chemical composition of metal powder cored wire is shown in table 1.

Table 1. Chemical composition of metal powder cored wire (wt.%).

B	C	Mn	Si	P	S	Fe
5.91	0.13	1.75	0.75	0.02	0.01	Bal
5.84	0.57	1.77	0.72	0.03	0.02	Bal
5.86	0.97	1.76	0.76	0.02	0.02	Bal

Firstly, the surfacing samples prepared from different carbon content metal powder cored wires were heat treated at 800 °C for 48 h. Then, specimens with size 10 mm× 10 mm × 10 mm were cut off from the middle of the surfacing plate by electrical discharge wire-cutting. The standard metallographic preparation using silicon carbide abrasive paper from 150 to 1200 grit was prepared, and then was polished with diamond compound polishing paste with 2.5 mm diamond particle size on a nylon cloth. The phase structure of the surfacing alloy was analyzed by X-ray diffraction with a D/max-2500/PC diffractometer equipped with Cu-Kα radiation, with the scanning range $20° \leq 2\theta \leq 90°$ and a step size of 0.02° and the dwell time was 2 s. After etched with a solution of 5 g $FeCl_3$ + 10 ml HNO_3 + 3 ml HCl + 87 ml ethylalcohol, the microstructure was analyzed by using an Axiovert 200 MAT optical microscope. The thermal stability of the Fe_2B hard phase was investigated by the above analytical test methods.

3. Experimental results and analysis

3.1. Microstructure of high boron surfacing alloy

As can be seen from the observation in figure 1, when the boron content is a hypereutectic alloy, a large number of massive and long-shaped primary Fe_2B structures are precipitated, and the bulk structure of the bulk structure is relatively large, and has a slender rod-like structure with a flat interface. If the rod-like structure is observed from the section to a regular square, rectangular or L-shape, the volume fraction is determined by the boron content and is independent of the carbon content. The microstructure of a large number of massive and long-grained primary Fe_2B precipitated in the microstructure of low-carbon and high-boron surfacing welds did not change after 800 °C and 48h heat treatment, and the block, long strips remained. The matrix Fe in the eutectic structure between the rod-shaped Fe_2B is oxidized by heat treatment. However, the microstructure of the eutectic structure Fe_2B in the matrix did not change.

As can be seen from the observation in figure 2, when the boron content is a hypereutectic alloy, the microstructure is bulk primary Fe_2B. A large amount of eutectic structure is distributed between the rod-like tissues. When the carbon is 0.57 wt%, the eutectic structure is fishbone Fe_2B+γ-Fe and a small amount of chrysanthemum $Fe_3(C,B)$. The primary Fe_2B microstructure of the medium-carbon high boron surfacing welds did not change after 800 °C, 48 h, still maintained a rod shape. But the eutectic structure between the primary crystal Fe_2B changed greatly, the fishbone and

chrysanthemum eutectic structure disappears. It can be clearly observed that the matrix Fe is oxidized, and the chrysanthemum-like Fe_3(C,B) is decomposed.

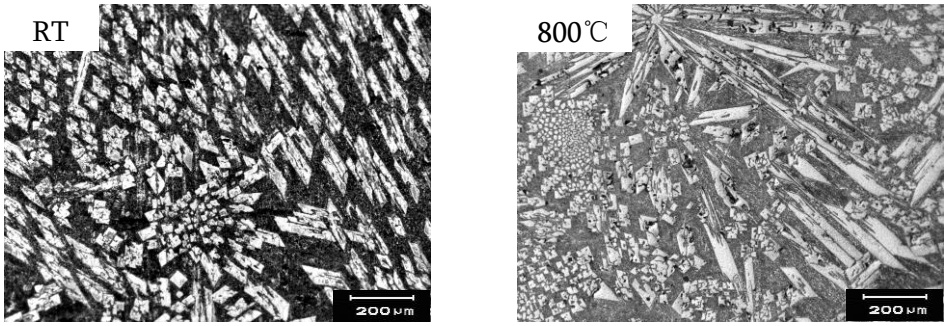

Figure 1. Microstructure of low carbon high boron surfacing alloy.

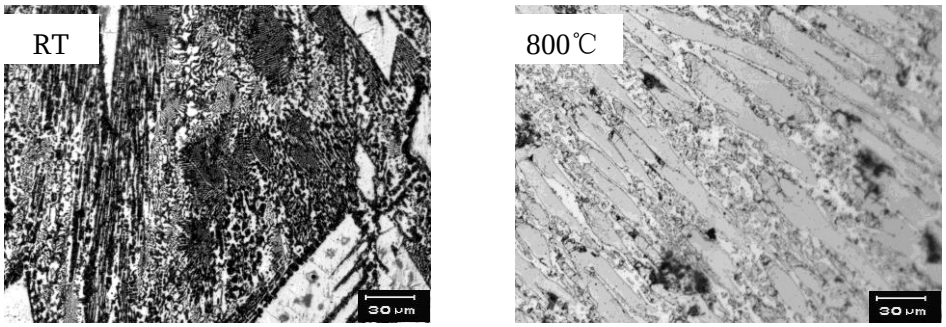

Figure 2. Microstructure of medium carbon high boron surfacing alloy.

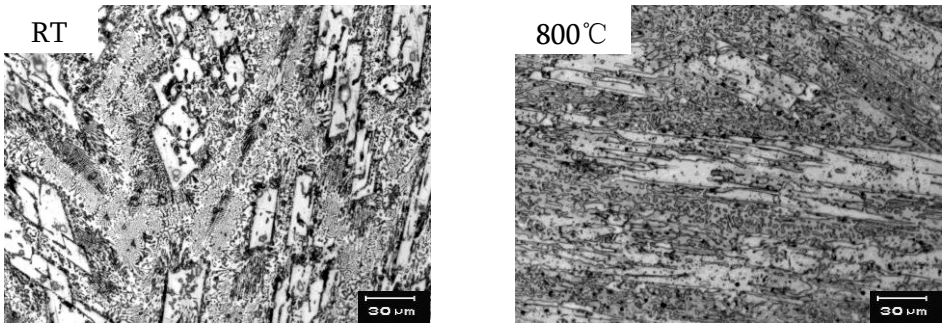

Figure 3. Microstructure of high carbon high boron surfacing alloy.

As can be seen from the observation in figure 2, when the boron content is a hypereutectic alloy, the microstructure is primary crystal Fe_2B, which is square and rectangular, and a large amount of eutectic structure is distributed between the rod-like structures. The carbon content is 0.57 wt%, and fish bone-like structure and a small amount of chrysanthemum-like structure are precipitated in the surfacing alloy. When the carbon content is 0.97 wt%, the fish bone tissue disappears and the eutectic structure consists of chrysanthemum tissue, as shown in figure 3. It can be seen that the structure of the eutectic structure depends on the content of elemental carbon in the surfacing alloy. The low carbon is the fish bone eutectic structure, the carbon content is increased, and the eutectic structure is transformed into the chrysanthemum tissue. The primary Fe_2B in the high carbon and high boron surfacing weld is still rod-like after 800 °C, 48 h heat treatment. But the chrysanthemum eutectic Fe_3(C,B) distributed between the rod-shaped Fe_2B disappeared. The eutectic structure Fe_3(C,B) is unstable and undergoes oxidative decomposition. It can be seen from the above analysis that the primary crystal Fe_2B in the high carbon high boron surfacing weld has good thermal stability, and the eutectic structure has a poor thermal stability.

3.2. XRD pattern of surfacing alloy

XRD diffraction of surfacing alloys with different compositions is shown in figures 4-6. The phase composition of the high boron iron based surfacing alloy is γ-Fe, Fe_2B and $Fe_3(C,B)$. The diffraction peaks of Fe and $Fe_3(C,B)$ are completely consistent with the peak intensity of the standard PDF card peak. The peak position of the diffraction peak of Fe_2B is consistent, but the peak intensity of the diffraction peak is abnormal, especially the carbon intensity of the sample is 0.57 wt%, 0.97 wt%, and the relative intensity of the (002) crystal plane diffraction peak of the diffraction angle $2\theta=42.527^o$ increases. The results show that the (002) crystal plane of a large amount of Fe_2B phase in the sample participates in diffraction.

The diffraction peak intensity of each phase in the high boron iron based weld surfacing alloy is related to the relative content of boron and carbon. The peak intensity of the diffraction peak of Fe_2B becomes stronger and sharper with the increase of boron content, and the corresponding diffraction peak of Fe gradually decreases. The diffraction peak of $Fe_3(C,B)$ only appears in the carbon content of 0.55 wt%, and the diffraction peak of $Fe_3(C,B)$ increases with the increase of carbon content.

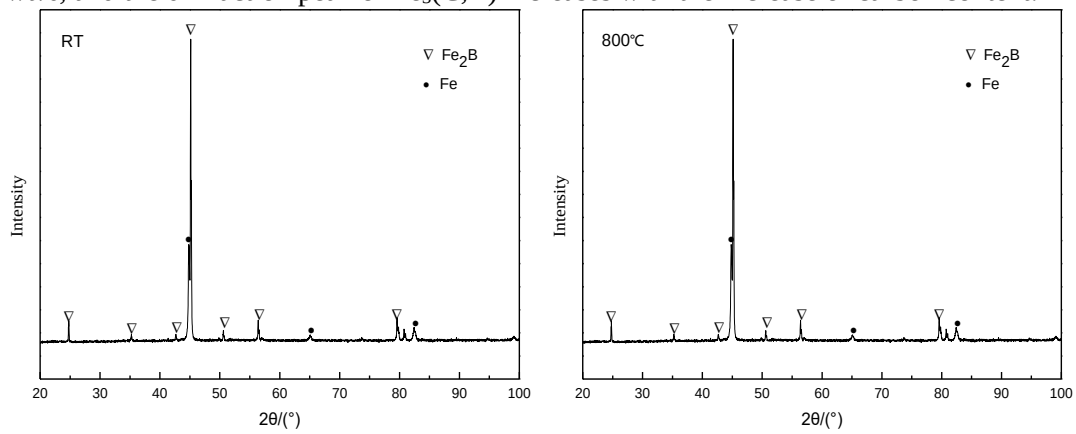

Figure 4. XRD patterns of low carbon high boron surfacing alloy before and after heat treatment.

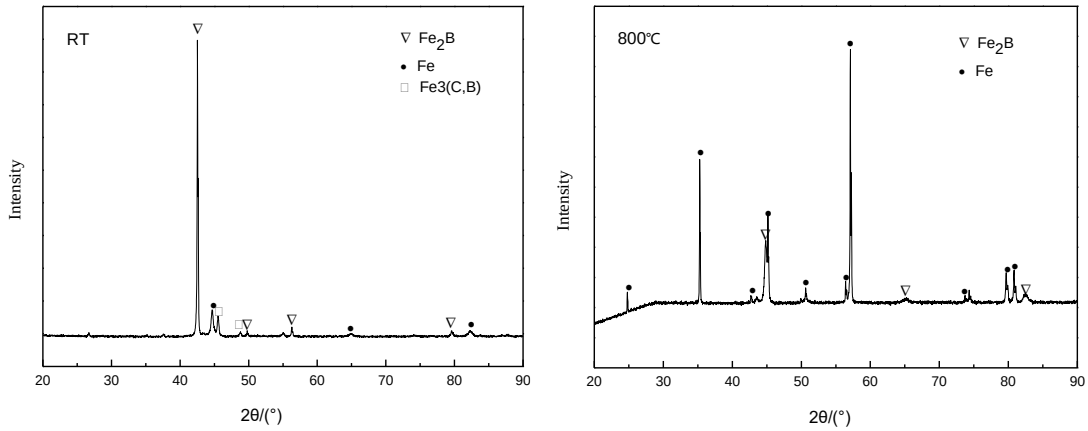

Figure 5. XRD patterns of medium carbon high boron surfacing alloy before and after heat treatment.

After 800 °C, 48 h, the phase composition of the low carbon high boron surfacing alloy is still γ-Fe and Fe_2B. The phase composition of the medium carbon high boron surfacing alloy is changed from γ-Fe+Fe_2B+eutectic $Fe_3(C,B)$ to γ-Fe+Fe_2B. The phase composition of Fe_2B, high carbon and high boron surfacing alloy is changed from γ-Fe+Fe_2B+eutectic $Fe_3(C,B)$ to γ-Fe+Fe_2B. It can be seen from the above that Fe_2B has good thermal stability, but $Fe_3(C,B)$ has poor thermal stability and is susceptible to oxidative decomposition at high temperatures.

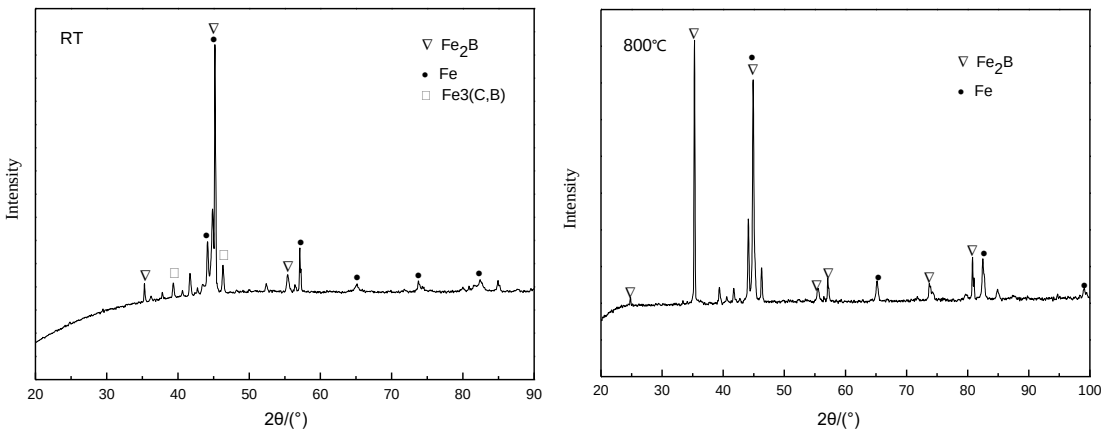

Figure 6. XRD patterns of high carbon high boron surfacing alloy before and after heat treatment.

4. Conclusion

When the carbon content is 0.13 wt%, the microstructure is blocky and rod-shaped Fe_2B+γ-Fe. When the carbon content is 0.57 wt%, the microstructure is a bulk Fe_2B+eutectic fishbone Fe_2B, and a chrysanthemum-like $Fe_3(B,C)$. When the carbon content increased to 1.0 wt%, the microstructure was blocky Fe_2B and eutectic structure chrysanthemum $Fe_3(B,C)$. The eutectic structure depends on the content of elemental carbon in the surfacing alloy, the low carbon is the fish bone eutectic structure, the carbon content is increased, and the eutectic structure is transformed into the chrysanthemum tissue. After heat treatment, the microstructure of the hard phase Fe_2B in the weld microstructure did not change, and remained in a block shape and a strip shape. Due to the high temperature effect, the eutectic fish bone structure Fe_2B+γ-Fe and the eutectic chrysanthemum $Fe_3(B,C)$+γ-Fe between the rod-shaped Fe_2B are converted into Fe_2B. Fe_2B hard phase has good thermal stability.

Acknowledgments

The work was supported by Heilongjiang Province Undergraduate Youth Creative Talents Training Program (UNPYSCT-2016203); Heilongjiang Natural Science Foundation Project (E2016067); Jiamusi University Provincial University Basic Research Business Expenses Project (2017-KYYWF-0605).

References

[1] Larsen-Badse, J., Mathew, K.G. (1969) Influence of structure on the abrasion resistance of a 1040 steel. Wear., 14: 199-205.
[2] Yao, M.X., Wu, J.B.C., Xie, Y. (2005)Mater. Sci. Eng, A., 407: 234-244.
[3] Speich, G.R. (1981) Physical metallurgy of dual-phase steels. In: Davenport, A.T. (ed.) Fundamentals of Dual-Phase Steels, The Metallurgical Society of AIME, Warrendale. pp. 1-45.
[4] Modi, O.P., Prasad, B.K., Jha, A.K., Das, S., Yegneswaran, A.H. (1994) Abrasive wear behaviour of an AISI 5132 steel under low stresses. Mater Trans JIM., 35: 67-73.
[5] Modi, A.P. (2006) Effect of microstructure and experimental parameters on high stress abrasive wear behaviour of a 0.19% wt C dual phase steel. Tribol. Int., 40: 490-497.
[6] Hurricks, P.L. (1973) Some metallurgical factors controlling the adhesive and abrasive wear resistance of steels. A review. Wear., 26: 285-304.
[7] Davies, R.G., Magee, C.L. (1979) Physical metallurgy of automotive high strength steels. In: Kott, R.A. (ed.) Structure and Properties of Dual Phase Steels, TMS-AIME., New York. pp. 1-29.
[8] Nakota, K., Araki, K., Kurihara, K. (1979) Physical metallurgy of dualphase steels. In: Davenport, A.T. (ed.) Formable HSLA and Dual Phase Steels, p. 183. TMS-AIME, New

York. pp. 181-203.
[9] Moore, M.A. (1974) The relationship between the abrasive wear resistance, hardness and microstructure of ferritic materials. Wear., 28: 59-68.
[10] Prasad, B.K., Prasad, S.V. (1991) Abrasion-induced microstructural changes during low stress abrasion of a plain carbon (0.5% C)steel. Wear., 151: 1-12.
[11] Modi, O.P., Prasad, B.K., Jha, A.K., Das, S., Yegneswaran, A.H. (1994) Abrasive wear behaviour of an AISI 5132 steel under low stresses. Mater Trans JIM., 35: 67-73.
[12] Allen, C., Ball, A. (1996) A review of the performance of engineering materials under prevalent tribological and wear. Tribol. Int., 2: 105-116.
[13] Davenport, A.T. (1977) Formable HSLA and Dual Phase Steels. American Institute of Mining, Metallurgical, and Petroleum Engineers., New York. pp. 65-78.
[14] Badisch, E., Krichgassner, M., Polak, R., Franek, F. (2008) The comparison of wear properties of different Fe-based hardfacing alloys in four kinds of testing methods. Tribotest., 14: 225-233.
[15] Badisch, E., Mitterer, C. (2003) Abrasive wear of high speed steels:influence of abrasive particles and primary carbides on wear resistance. Tribol. Int., 36: 765-770.
[16] Bressan, J.D., Baros, D.P., Sokolwski, A., Mesquita, R.A., Barbosa, C.A. (2008) Influence of hardness on the wear resistance of 17-4 PH stainless steel evaluated by the pin-on-disc testing. J. Mater. Process. Technol., 205: 353-359.
[17] Francucci, G., Sikora, J., Dommarco, R. (2008) Abrasion resistance of ductile iron austempered by the two step process. Mater. Sci.Eng., 485: 46-54.
[18] Kassim, S.R. (2000) Equivalent hardness concept and two-body abrasion of iron-base alloys. Wear., 243: 92-100.
[19] Celik, O., Ahlatci, H., Kayali, E.S., Cimenoglu, H. (2005) High temperature abrasive wear behavior of an as-cast ductile iron. Wear., 258: 189-193.
[20] Straffelini, G., Trabucco, D., Molinari, A. (2001) Oxidative wear of heat-treated steels. Wear., 250: 485-491.